Performance and cellular capacity of M-ary PSK in co-channel interference

Abstract—**Fast simulation techniques are applied to evaluate accurately the error rates of coherent M-ary phase shift keying (PSK) in the presence of co-channel interference (CCI) and additive white Gaussian noise (AWGN). This type of interference occurs often in wireless systems that employ frequency reuse. Error rates are frequently calculated based on the assumption that CCI can be modelled as Gaussian. It is shown that this assumption is valid only in noise dominated environments. Simulation techniques based on adaptive importance sampling (IS) are developed for this problem. Several new numerical results are presented which are used to calculate the cellular capacities of wireless systems.**

Keywords— **Importance Sampling, Co-channel interference, M-ary PSK, Cellular capacity.**

I. Introduction

MANY digital communication systems are perturbed by interference that can be modelled as a sum of sinusoids with random phases. Mobile wireless systems often operate in interference dominated environments which can have a limiting effect on performance in terms of bit error rates and cellular capacities. In particular, CCI in such systems arises from frequency reuse in certain fixed patterns of geographic cells, [1]-[2]. The information bearing signal in a particular frequency cell is interfered by signals arriving from surrounding cells that use the same frequency. These interfering signals appear with random phases in an additive manner, giving rise to CCI.

Performance analysis in terms of bit or symbol error rates is usually carried out by making the simplifying assumption that CCI can be modelled as being Gaussian. This assumption yields accurate results only when the signal to (additive white Gaussian) noise ratios are low compared to the corresponding signal to interference ratios. Hence more accurate methods are required in interference dominated situations wherein the combination of Gaussian noise and interference is decidedly non-Gaussian. One fast simulation method, based on adaptive IS [3] - [5], is developed in this paper for the coherent detection of M-ary PSK signalling. It is known that properly designed IS simulations can provide remarkable gains over Monte Carlo procedures in terms of computational effort for the estimation of rare event probabilities. In the following sections we adopt a simple structure for CCI, develop biasing methods for the random phases of the interferers and noise, describe implementation of adaptive estimators, present symbol error rates, and calculate cellular capacity for M- ary PSK. All analyses are carried out for interference dominated situations as well as those consisting of interference and additive white Gaussian noise (AWGN) in nonfading channels. However, binary and M-ary PSK are treated separately.

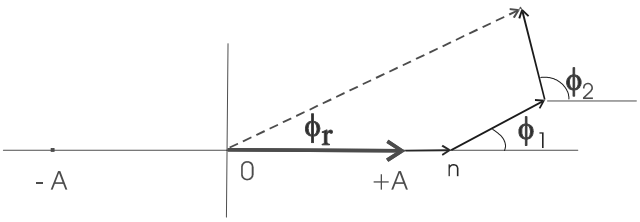

Fig. 1. Binary PSK signal space with 2 co-channel interferers and AWGN

II. Co-channel interference

The following assumptions are made on the interfering signals:

• The carrier signal amplitude of the desired information bit stream is A and the amplitude of the interfering signals is $\alpha\, A$ where α is a positive constant. The L interferers are assumed to have equal amplitudes.

• Interfering signals are assumed to be similarly modulated as the desired signal but carrying different equally likely information bits.

• The i-th interfering signal differs in phase from the desired signal by ϕ_i. The set $\{\phi_i\}_1^L$ consists of random independent phases, uniformly distributed in $(0, 2\pi)$. The interfering carriers are at the same frequency as the desired signal. It is also assumed that the interfering signals are bit synchronized with the desired signal, resulting in all the energy of the interferer appearing at the demodulator output. This represents a worst-case situation.

III. Binary PSK

The optimum receiver for coherent PSK is a correlation detector or a matched filter-sampler followed by a zero threshold decision. The signal space diagram in Figure 1 shows the receiver decision region for a transmitted $+1$ information bit with two interferers and AWGN. The decision statistic at the output of the demodulator with L interferers is proportional to

$$A + n + \sum_{i=1}^{L} \alpha A \cos\phi_i$$

where n is Gaussian and has zero mean with variance σ_n^2. The error probability can therefore be written as

$$\begin{aligned} P_e &= P(A + n + \sum_{i=1}^{L} \alpha A \cos\phi_i \le 0) \\ &= E\{1(A + n + \sum_{i=1}^{L} \alpha A \cos\phi_i \le 0)\} \end{aligned}$$

where the indicator function $1(\cdot) = 1$ if the event in its argument occurs and is zero otherwise. Each cosine term in the above has the probability density function shown as the solid line in Figure 2. Calculating the density of their sum is a computationally intensive task, involving an L-fold convolution. Assuming that the sum can be characterized by an equivalent Gaussian density (based on the central limit theorem) leads to

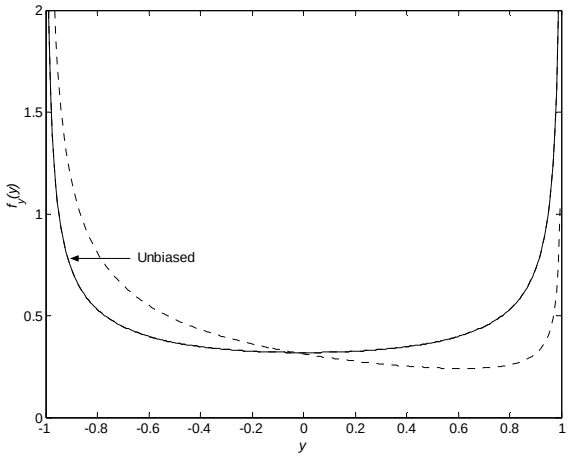

Fig. 2. Pdf of a random phase interfering signal

inaccurate answers, as is shown later. While there exists an analytical approximation for the sum density [6], it is advantageous to resort to IS simulation to estimate P_e. This method is general and is applicable to a broad class of performance estimation problems. The IS estimator $\widehat{P}_e$ of P_e is given by

$$\widehat{P}_e = \frac{1}{K}\sum_{k=1}^{K} 1(A+n+\sum_{i=1}^{L}\alpha A\cos\phi_i \le 0) \cdot W(\phi_1,\ldots,\phi_L,n), \qquad f\sim f_\star \tag{1}$$

where the notation "$f \sim f_\star$" is used to signify that the K-length simulation is carried out with the original densities (f) of the random variables involved in the indicator replaced by biasing densities ($f_\star$) that cause the error event to happen more often. The weighting function W ensures that the estimates are unbiased. The biasing densities are chosen such that the variances of the estimates are smaller than those that would be obtained without any biasing for a conventional Monte Carlo simulation of equal length.

We consider the biasing of the interference phases and additive noise separately. The interference cosine terms need to have increased probability mass in the negative regions of the support of the density. To achieve this an effective way to bias the phases ϕ_i is to increase the probability mass in the vicinity of $\phi_i = \pi$. We use a Gaussian biasing density with mean at π and a common variance of σ_ϕ. An example of the biased density for $\cos\phi$ is also shown as a dashed line in Figure 2 for $\sigma_\phi = 1.5$. Of course, the Gaussian simulation samples that fall outside the $(0, 2\pi)$ interval are wasted, but it turns out that the consequent loss in efficiency is small.

For biasing the noise n, it is clear that endowing it with a negative mean would increase the probability of making detection errors. While variance scaling can be used, in this case it will not be as efficient as translating the mean. Denoting translation with parameter c, the weighting function is easily shown to be

$$W(\phi_1,\ldots,\phi_L,n;\sigma_\phi,c) \equiv \frac{f(\phi_1,\ldots,\phi_L,n)}{f_\star(\phi_1,\ldots,\phi_L,n;\sigma_\phi,c)} = \begin{cases} \left(\frac{\sigma_\phi}{\sqrt{2\pi}}\right)^L \exp\left(\frac{\sum_1^L(\phi_i-\pi)^2}{2\sigma_\phi^2} + \frac{c^2-2c\,n}{2\sigma_n^2}\right), & 0\le\phi_i\le 2\pi \\ 0, & \text{elsewhere} \end{cases} \tag{2}$$

To implement the estimator of (1) it remains to choose good values of the biasing parameters σ_ϕ and c. This is done in an adaptive two-dimensional optimization that determines optimum values of the parameters such that the variance of the estimator is minimized. Such procedures have been adequately described in [4] and [5]. They use stochastic Newton recursions that require the partial and mixed derivatives $\partial W/\partial\sigma_\phi$, $\partial W/\partial c$, $\partial^2 W/\partial\sigma_\phi^2$, $\partial^2 W/\partial c^2$, and $\partial^2 W/\partial\sigma_\phi\partial c$. All these are easily obtained from (2). The IS optimization algorithm is the stochastic Newton recursion

$$\begin{pmatrix}\sigma_{\phi,m+1}\\ c_{m+1}\end{pmatrix} = \begin{pmatrix}\sigma_{\phi,m}\\ c_m\end{pmatrix} - \delta\widehat{\boldsymbol{J}}_m^{-1}\cdot\widehat{\nabla}I(\sigma_{\phi,m},c_m), \quad m=1,2,\ldots$$

where δ is the step size of the recursion and $\widehat{\boldsymbol{J}}_m^{-1}$ is the inverse of the matrix $\widehat{\boldsymbol{J}}_m$ given by

$$\widehat{\boldsymbol{J}}_m = \begin{pmatrix}\hat{I}_{\sigma_{\phi,m}\sigma_{\phi,m}} & \hat{I}_{\sigma_{\phi,m}c_m}\\ \hat{I}_{\sigma_{\phi,m}c_m} & \hat{I}_{c_mc_m}\end{pmatrix}$$

where $I_{xy} \underline{\Delta} \partial I_x/\partial y$. The estimated gradient operator $\widehat{\nabla}$ is

$$\widehat{\nabla}I(\sigma_{\phi,m},c_m) = (\hat{I}_{\sigma_{\phi,m}} \quad \hat{I}_{c_m})^T$$

where $I_{\sigma_{\phi,m}} = \partial I(\sigma_{\phi,m},c_m)/\partial\sigma_{\phi,m}$ and $I_{c_m} = \partial I(\sigma_{\phi,m},c_m)/\partial c_m$, and

$$I(\sigma_{\phi,m},c_m) = E\{1(A+n+\textstyle\sum_{i=1}^L\alpha A\cos\phi_i\le 0)\,W(\phi_1,\ldots,\phi_L,n)\}$$

is a quantity that is proportional to the estimator variance, the expectation being taken over the unbiased distributions. All terms with hats are estimates obtained during the IS simulation as part of the optimization algorithm. Simulations have been carried out for $L = 6$ interferers. This is an example of a wireless mobile communications network with a hexadiagonal cell structure in which interfering cells use the same frequency as the cell under study. The 6 cells closest to the cell under study are at an equal distance while all other cells using the same frequency are at a larger distance and assumed to contribute negligible interference compared to the first tier. In the absence of noise, the signal to interference ratio SIR is defined as $1/L\alpha^2$. Shown in Figure 3 is the algorithm for σ_ϕ for an SIR of 7.615dB which corresponds to a P_e of 10^{-6}. For an IS sample size of $K = 10,000$, the gain over conventional Monte Carlo simulation obtained is 7.4×10^5 at a bit error rate of 10^{-6}. This provides a relative accuracy better than 2.5% for a confidence level of 95%. The P_e estimates are shown in Figure 4. It is observed that for SIR values higher than 7.81 dB, the error probability becomes zero and no bit errors occur due to interference. This corresponds to $\alpha = 1/6$. This simply

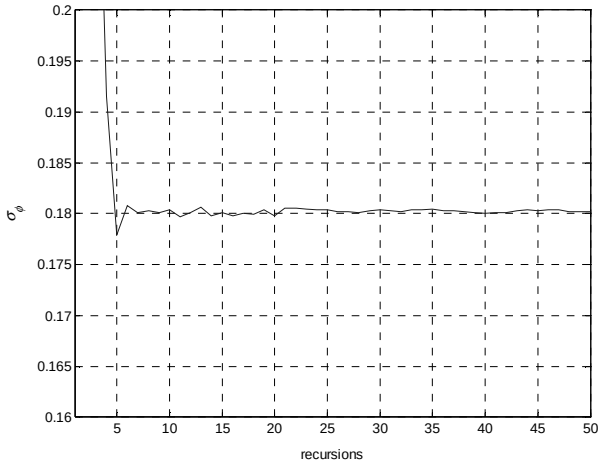

Fig. 3. Convergence of variance parameter for SIR=7.615 dB and $P_e = 10^{-6}$

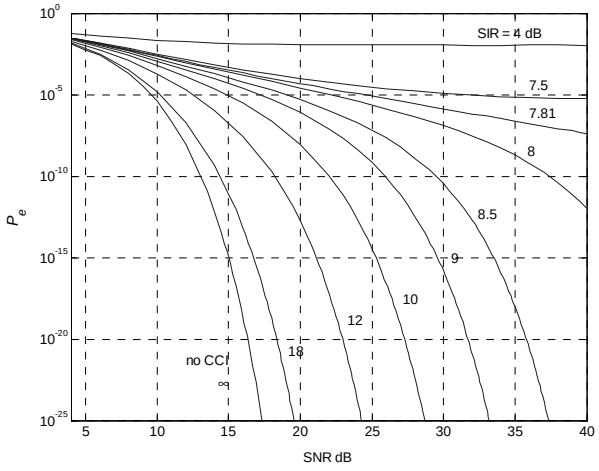

Fig. 5. Error probabilities for BPSK with CCI and AWGN. Parameter is SNR

means that for any $\alpha < 1/L$ the maximum possible total vector length of L interferers cannot exceed the signal vector length. Thus there exists, for the interference dominated situation, a zero error threshold of signal to interference ratio above which no bit errors are possible. In the presence of AWGN, the signal

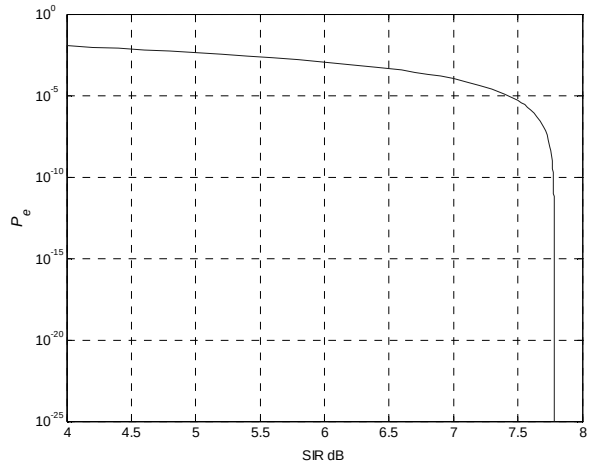

Fig. 4. BER of BPSK receiver calculated with Adaptive Importance Sampling

to noise ratio is defined as SNR $= A^2/2\sigma_n^2$. Results are shown in Figure 5 and 6. For an SIR of 8.5dB and SNR of 29dB, a simulation gain of 8.6×10^8 at an error rate of 2.4×10^{-10} is obtained. A relative accuracy better than 6.6% for P_e estimation is obtained for all cases. The bit error probability is shown in Figure 5 as a function of SIR with SNR as parameter. For finite SNR an error floor exists as the SIR becomes large. The same result is shown in Figure 6 but with SIR as the parameter. For all SIR < 7.81dB, which is the zero error threshold for CCI, an error floor exists as SNR $\to \infty$. Above this threshold value of SIR, there is no floor.

A. Gaussian assumption

The effect of modelling the CCI as Gaussian is examined by calculating the bit error rate assuming that the interference can

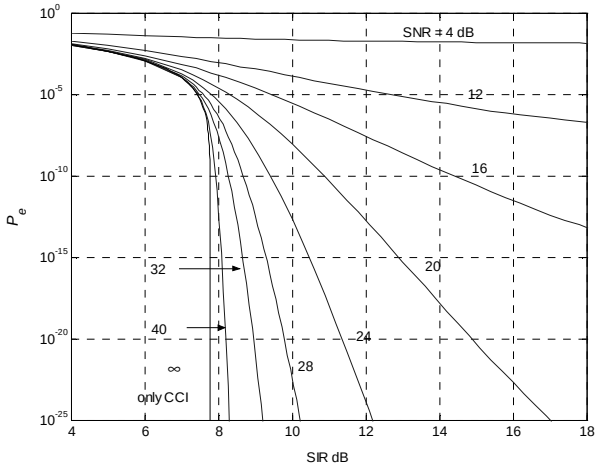

Fig. 6. Error probabilities for BPSK with CCI and AWGN. Parameter is SIR

be replaced by a Gaussian noise source having the same total power, in addition to thermal noise of course. Defining a signal to interference and noise ratio SNIR as

$$\text{SNIR} = \frac{A^2}{L\alpha^2 A^2 + 2\sigma_n^2}$$

the error rate is approximated as

$$P_e \approx Q\big(\sqrt{2\,\text{SNIR}}\big)$$

where $Q(x) \equiv \int_x^\infty e^{-y^2/2}\,\mathrm{d}y/\sqrt{2\pi}$. This is shown in Figure 7, together with optimized IS estimates of P_e for comparison. For low SNRs, that is in noise dominated situations, the Gaussian approximation is close to the IS estimates. As the SNR increases, in the interference dominated situation, the approximation becomes increasingly worse. This illustrates the importance of making accurate simulation estimates of performance in interference limited environments in preference to using Gaussian approximations.

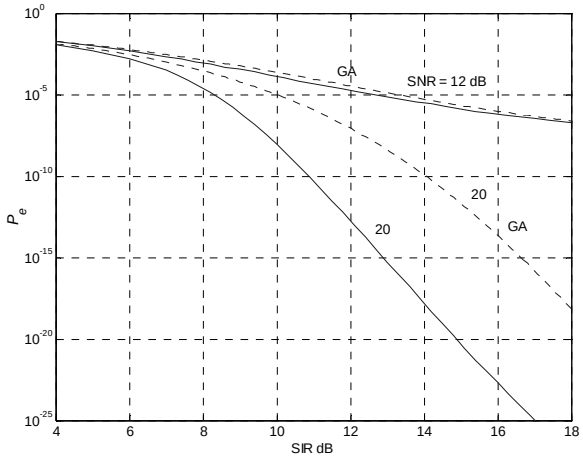

Fig. 7. Comparison of Gaussian approximations (GA) and IS simulation for BPSK

IV. M-ary PSK

For transmitting M-ary symbols using PSK, $\log_2 M$ information bits are encoded into each symbol waveform in terms of the phases of the carrier. The optimum receiver is equivalent to a phase detector that computes the phase of the received signal vector and selects that symbol whose phase is closest. Assume that zero phase has been transmitted. From the signal space diagram of Figure 8, in which $L = 1$, the phase ϕ_r of the received vector is described by

$$\sin\phi_r = \frac{n_q+\alpha A\sum_{i=1}^{L}\sin\phi_i}{\sqrt{\left(n_q+\alpha A\sum_{i=1}^{L}\sin\phi_i\right)^2+\left(n_i+A+\alpha A\sum_{i=1}^{L}\cos\phi_i\right)^2}} \tag{3}$$

and

$$\cos\phi_r = \frac{n_i+A+\alpha A\sum_{i=1}^{L}\cos\phi_i}{\sqrt{\left(n_q+\alpha A\sum_{i=1}^{L}\sin\phi_i\right)^2+\left(n_i+A+\alpha A\sum_{i=1}^{L}\cos\phi_i\right)^2}} \tag{4}$$

where n_i and n_q denote the inphase and quadrature noise components. A correct detection is made when ϕ_r satisfies $-\pi/M \le \phi_r \le \pi/M$. Defining $\overline{1}(\cdot) = 1 - 1(\cdot)$, the probability of a symbol error can be written as

$$\begin{aligned} P_e &= P(-\pi/M \not\le \phi_r \not\le \pi/M) \\ &= E\{\overline{1}(-\pi/M \le \phi_r \le \pi/M)\} \end{aligned}$$

and its IS estimate as

$$\widehat{P_e} = \frac{1}{K}\sum_{k=1}^{K}\overline{1}(-\pi/M \le \phi_r \le \pi/M)\, W(\phi_1,\ldots,\phi_L,n_i,n_q)$$

The indicator for the complement of the event $\{-\pi/M \le \phi_r \le \pi/M\}$ can easily be simulated by referring to the signal space diagram of Figure 8 and noting that the error region comprises of the region $\{n_i + A + \alpha A\sum_{i=1}^{L}\cos\phi_i \le 0\}$ together with (union) the intersection

$$\{n_i + A + \alpha A\textstyle\sum_{i=1}^{L}\cos\phi_i > 0\} \cap \{\{\tan\phi_r \ge \tan(\pi/M)\} \cup \{\tan\phi_r \le -\tan(\pi/M)\}\}$$

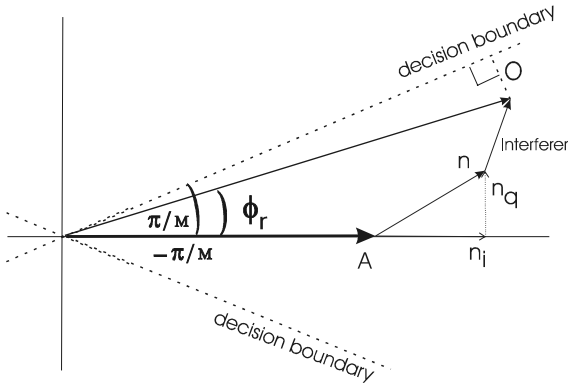

Fig. 8. M-ary PSK signal space with a single co-channel interferer and AWGN

Further, we note that the distribution of the received phase ϕ_r is symmetric around $\phi_r = 0$ by virtue of the fact that all the interference phases are independent and uniformly distributed, the same being true for the phase of the noise vector. Hence it is sufficient to simulate events from only (the upper) half of the error region described above. This in turn can be described by considering the intersection of the complete error region and the set $\{\sin\phi_r \ge 0\}$.

Consequently, an effective method of biasing is to generate all interference phases ϕ_i such that vectors are most likely to be aligned along the line marked O in Figure 8. This is evident from orthogonality and will produce an increase in the frequency of occurrence of errors. Hence the biased interfering phases are chosen as Gaussian with their means at $\mu \equiv (\pi/2)+\pi/M$ and common variance σ_ϕ, optimized through adaptive simulation. As far as the noise n is concerned, increasing its variance will of course produce more errors. However this will lead to a more than two-dimensional optimization problem. A simple solution is to translate the means of the quadrature noise variables along the shortest line to the decision boundary, as is done for the interferers. Denoting the biased means of the noise components as c_i and c_q, it follows from Figure 8 that they should be related as

$$c_i = -c_q \tan\frac{\pi}{M}$$

This results in a two-dimensional biasing problem involving the parameters c_i (or c_q) and σ_ϕ. The weighting function is

$$W(\phi_1,\ldots,\phi_L,n_i,n_q;\sigma_\phi,c_q) = \begin{cases} \left(\frac{\sigma_\phi}{\sqrt{2\pi}}\right)^L \exp\left(\frac{\sum_1^L(\phi_i-\mu)^2}{2\sigma_\phi^2} + \frac{(1+a^2)c_q^2+2c_q(an_i-n_q)}{2\sigma_n^2}\right), & 0 \le \phi_i \le 2\pi \\ 0, & \text{elsewhere} \end{cases}$$

where $a \equiv \tan(\pi/M)$. The various derivatives can easily be obtained. Simulations are carried out in a similar manner to the binary PSK case. Results are shown in Figures 9 and 10 for 8-PSK. The SNR per bit is defined as $A^2/(2\sigma_n^2\log_2 M)$ and the SIR as $1/(L\alpha^2\log_2 M)$. The symbol error rate performances for QPSK differ only slightly from those for binary PSK and are not shown. The same general remarks on error rate performance can be made as in the case of binary PSK.

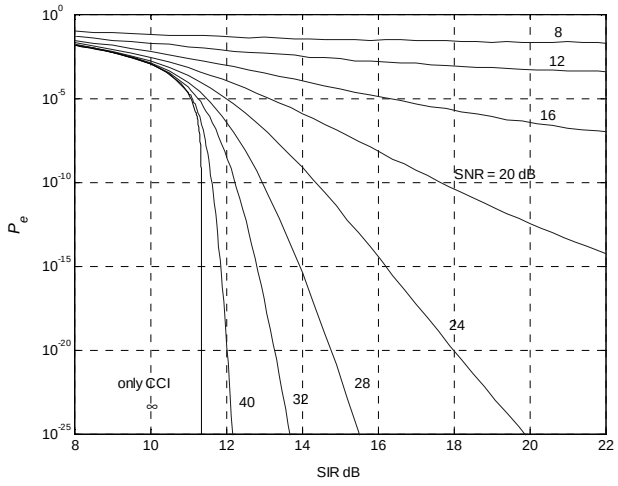

Fig. 9. Error probabilities for 8-PSK with CCI and AWGN. Parameter is SNR

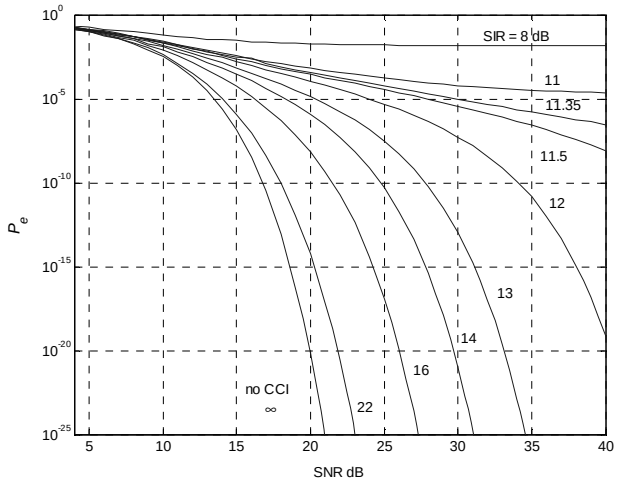

Fig. 10. Error probabilities for 8-PSK with CCI and AWGN. Parameter is SIR

A. Capacity

Based on IS estimates of error rates, we can find the capacity per hexadiagonal cell for M-ary PSK. To calculate the capacity per cell as a function of the SNR, SIR and error rate, a few more parameters need to be defined. We will choose some commonly used, realistic parameter values. The required bandwidth is set to the null-to-null bandwidth. Hence, the bandwidth efficiency η for M-ary PSK is $\eta = \frac{1}{2}\log_2 M$. In the hexadiagonal structure, the number of cells in a reuse pattern is denoted by the reuse factor K_{cell}. The cell structure only allows for a set of values given by $K_{\text{cell}} = i^2 + ij + j^2$, where i and j are two non-negative integers [2]. A common method to achieve a performance better than some specified error rate is to increase the ratio D/R, where D is defined as the distance between the centers of two co-channel cells and R as the cell radius. The D/R ratio is related to the SIR as

$$\text{SIR} = \frac{1}{6}\left(\frac{D}{R}\right)^{\gamma} \tag{5}$$

where γ is the path loss exponent. The relation between D/R and K_{cell} can be easliy found by using the fact that the perpendicular cell diameter is equal to $\sqrt{3}R$. This results in the relation $D/R = \sqrt{3K_{\text{cell}}}$. A path loss exponent $\gamma = 4$ is commonly used. Substituting these relations in (5) yields $\text{SIR} = \frac{3}{2}K_{\text{cell}}^2$. Finally, the capacity per cell is defined as the ratio $C = \eta/K_{\text{cell}}$. Substitution yields

$$C = \frac{\frac{1}{2}\log_2 M}{\sqrt{\frac{2}{3}\text{SIR}}} \qquad \text{[bits / s / Hz / cell]} \tag{6}$$

To compare M-ary PSK modulation schemes, it is assumed that all symbols are equally likely and use Gray encoding. Hence, errors that occur over more than one signal point are negligible compared to errors that occur over a single signal point. Also, the symbol error rate is well approximated by the bit error rate.

The following procedure is used to find the capacity per cell as a function of the BER. For a specified SNR and BER, the lowest SIR is found that satisfies the BER condition. The capacity per cell then follows from (6). Since K_{cell} only takes non-negative integer values, the capacity per cell takes discrete values. The results are shown for BPSK, QPSK and 8-PSK in Figures 11-13. The capacity per cell is presented in two ways. First, as a continuous function of the BER, ignoring the fact that K_{cell} only takes non-negative integer values. Second, as a discrete function of the BER, taking into account that $K_{\text{cell}} \in \{1, 3, 4, 7, \ldots\}$. For clarity, the latter is only shown for SNR = 16 dB. Markers are placed on the continuous capacity graphs to indicate the transitions of K_{cell}. Reuse factors are indicated at the discrete capacity values, between parenthesis.

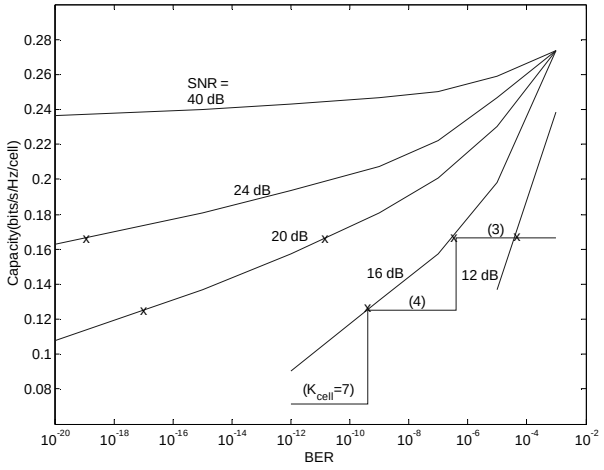

Fig. 11. Capacity per cell as a function of the required bit error rate for BPSK. Markers indicate the transitions of K_{cell}. K_{cell} values are in parenthesis. Parameter is SNR.

For most combinations of BER and SNR, QPSK provides the maximum capacity per cell. This is illustrated more explicitly for SNR = 16 dB in Figure 14. Comparing the discrete capacity values at SNR = 16 dB, we conclude that QPSK provides the highest capacity per cell for $10^{-12} \leq \text{BER} \leq 2 \cdot 10^{-4}$. QPSK is outperformed by 8-PSK in a small region $2 \cdot 10^{-4} \leq \text{BER} \leq 10^{-3}$. For higher SNR, the region in which 8-PSK outperforms

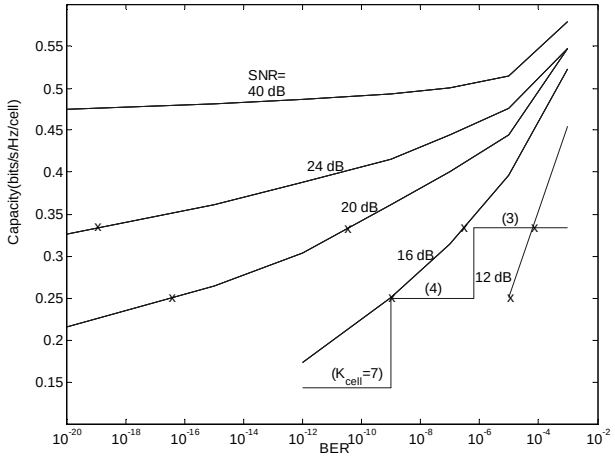

Fig. 12. Capacity per cell as a function of the required bit error rate for QPSK. Markers indicate the transition of K_{cell}. K_{cell} values are in parenthesis. Parameter is SNR.

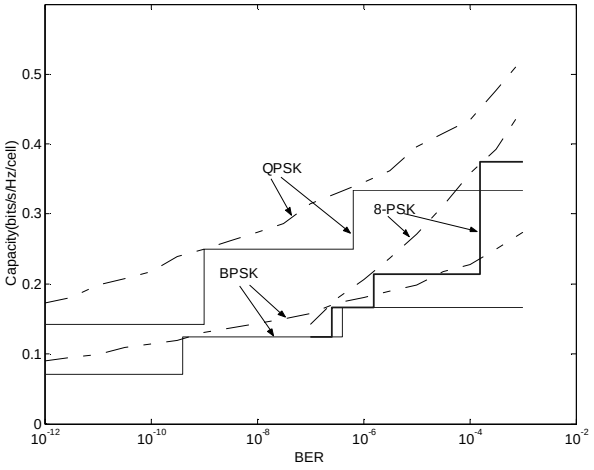

Fig. 14. Comparison of capacity per cell for SNR = 16 dB. Dashed lines represent the continuous capacity graphs. Solid lines represent the discrete capacity values.

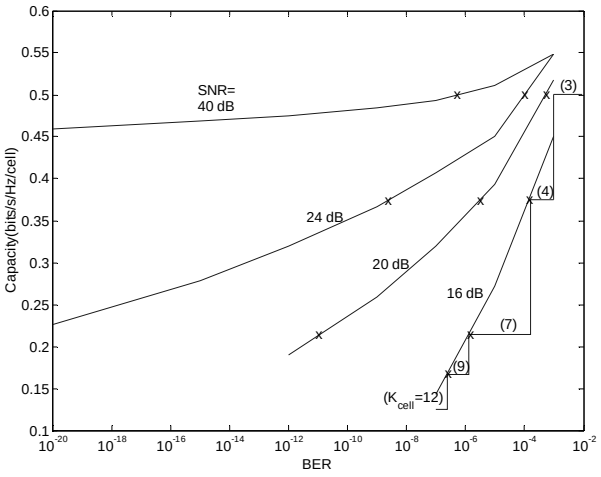

Fig. 13. Capacity per cell as a function of the required bit error rate for 8-PSK. Markers indicate the transition of K_{cell}. K_{cell} values are in parenthesis. Parameter is SNR.

QPSK extends towards lower BER. The opposite occurs for lower SNR. Furthermore, BPSK is outperformed by QPSK for any combination of BER and SNR.

V. Conclusion

In this paper we have demonstrated how adaptive importance sampling methods can be used to solve performance estimation problems that are analytically intractable. Such tasks would be computationally very intensive if one were to resort to conventional Monte Carlo simulations. Although numerical results were displayed only for M-ary PSK, results for other signal sets can easily be obtained. In particular, it has been shown that the assumption of a Gaussian model in an interference dominated situation is not justified for the purpose of evaluating error rates. Further, the techniques developed here can be applied to different modulation schemes as also to channels characterized by fading and multipath. The performance results are used to calculate the cellular capacity of wireless systems by incorporating propagation models and bandwidth considerations. It was found that QPSK outperforms BPSK and 8-PSK for most BER and noise levels. These results can be related to the work in [6]. Therein an interference dominated channel model was considered and Gaussian noise assumed absent. The analysis in [6] was based on a density approximation derived in [7] to estimate the error rates of various modulation schemes. By including Gaussian noise in the channel model, more realistic performance analysis and capacity results have been obtained.

References

[1] Feher, K.: *Wireless digital communications*, Prentice-Hall, New Jersey, 1995.

[2] Rappaport, T.S.: *Wireless communications: Principles and Practices*, Prentice-Hall, New Jersey, 1996.

[3] Remondo, D., Srinivasan, R., Nicola, V. F., Van Etten, W., and Tattje, H. E. P.: 'Adaptive importance sampling methods for performance evaluation and parameter optimization of communication systems,': *IEEE Transactions on Communications*, Vol. 48, No. 4, April 2000, pp 557-565.

[4] Srinivasan, R.: 'Simulation of CFAR detection algorithms for arbitrary clutter distributions,' *Proc. IEE, Radar, Sonar and Navigation*, Part F, Vol. 147, Issue 1, Feb 2000, pp 31-40.

[5] Srinivasan, R.: 'Some results in importance sampling and an application to detection,' *Signal Processing*, Feb 1998, vol 65, Issue 1, pp 73-88.

[6] Thijs, J., Haartsen, J., Srinivasan, R., and Van Etten, W.: 'Optimizing cell capacity for cellular systems,' *IEEE 8th Symposium on Communications and Vehucular Technology in the Benelux*, October 18, 2001, Delft, The Netherlands, pp 30-35.

[7] Srinivasan, R.: 'Estimation and approximation of densities of i.i.d. sums via importance sampling,' *Signal Processing*, Dec 1998, vol 71, Issue 3, pp 235-246.